Vortex dipole collision with a sliding wall

J E V Guzmán[1], L P J Kamp[2] and G J F van Heijst[2]

[1] National Autonomous University of Mexico, Institute for Materials Research,
Ciudad Universitaria 04510, Coyoacan, D. F., Mexico
[2] Department of Applied Physics, Eindhoven University of Technology, PO Box 513,
NL-5600 MB Eindhoven, The Netherlands

E-mail: eguzman@iim.unam.mx, L.P.J.Kamp@tue.nl and G.J.F.v.Heijst@tue.nl

Communicated by W Young

Abstract
The collision of a dipolar vortex with a sliding wall is investigated numerically.
Previous studies have shown that perpendicular vortex collisions with fixed
walls may lead to a rebound of the primary dipole during which the
symmetry of the vorticity field with respect to the dipole's axis is preserved.
However, a wall sliding tangentially breaks this symmetry, leading to
distinctive flow regimes for different wall speeds. The conditions for which
the transition between these two regimes occur are studied, both numerically
and analytically, in terms of the wall speed and the Reynolds number of the
dipolar flow.

(Some figures may appear in colour only in the online journal)

1. Introduction

The interaction of vortices with flat walls and other obstacles in a fluid is a fundamental
issue in fluid dynamics, and has been and still is being given much attention. The interest in
the subject is motivated by practical applications and also by the need to gain better insight
in the dynamics of vorticity interacting with obstacles. One of the canonical problems in
vortex–wall interaction is that of a dipolar vortex impinging perpendicularly on a no-slip flat
wall. This problem has been studied extensively, both numerically and experimentally, by
Orlandi (1990), Carnevale *et al* (1997) and by Kramer *et al* (2007). During such a collision,
secondary, oppositely signed vorticity is generated at the wall in order to satisfy the no-
slip boundary condition (see e.g. Doligalski and Walker (1984), Chuang and Conlisk (1989),
Peridier *et al* (1991a), (1991b) and Atassi *et al* (1997)). Typically, this secondary vorticity
may be combined with the primary vorticity in order to form two secondary dipoles that
propagate away from the wall along curved trajectories. A generic feature of such a rebound

is that the symmetry present in the initial vorticity field is preserved during the evolution of the flow. Other types of vortex–wall interaction that preserve symmetry and have been studied previously are that of a vortex dipole impinging on a cylinder (Orlandi 1993, Verzicco *et al* 1995) or on finite aspect-ratio rectangular shapes (Danaila 2004).

In many practical applications the symmetry in dipole–wall interactions may be broken for example when there is a cross-flow perpendicular to the path of the dipole or if the wall itself is moving. Cross-flow-induced asymmetry is, for example, important for the collision of aircraft-generated trailing vortices with a runway in a cross-wind. An early study by Zheng and Ash (1996) discusses this type of asymmetry that is present in the primary vortices generated by the aircraft itself and also in the boundary-layer vorticity induced by the cross-wind near the no-slip runway. Parameterizing the effects of such cross-winds on the temporal evolution of the dipole-runway collision is difficult (Holzäpfel and Steen 2007) and a serious concern. Moving wall-induced asymmetry is, for example, encountered when studying the flow inside a combustion chamber or the flow of blood inside the human heart (e.g. Loerakker *et al* 2008). Also, no-slip walls bounding two-dimensional (2D) domains have a decisive impact on evolving 2D turbulence in such domains. It is therefore to be expected that moving no-slip walls will modify the intriguing properties of confined 2D turbulence that are yet to be explored. The dipolar vortex constitutes one of the building blocks of such 2D turbulence and therefore can be used to gain insight in the asymmetry that results from the collision of such a vortex structure with a no-slip wall that is sliding parallel to itself at a constant speed. The present paper studies such a collision both numerically and analytically. Results of numerical simulations are presented for different wall speeds. We focus on the generic behavior observed during the collision, and thus identify two regimes for low and high wall speeds. The transition between these two regimes is analyzed numerically and analytically.

2. Problem formulation and numerical setup

This study is concerned with the interaction of a dipolar vortex with a sliding wall. To this end we consider the half-space $x \leqslant 0$ containing an incompressible fluid with viscosity ν and velocity field $\mathbf{v} = u\,\mathbf{e_x} + v\,\mathbf{e_y}$, where $\mathbf{e_x}$ and $\mathbf{e_y}$ are the unit vectors in the x- and y-direction, respectively. The geometry and the initial flow configuration are displayed in figure 1.

At time $t = 0$ the flow in this domain is initialized in the form of the Lamb–Chaplygin dipole extensively discussed by Meleshko and van Heijst (1994), which corresponds to a steady solution of the 2D Euler equations. The vorticity determined by

$$\omega = \mathbf{e_z} \cdot \nabla \times \mathbf{v}, \tag{1}$$

where $\mathbf{e_z} = \mathbf{e_x} \times \mathbf{e_y}$, is concentrated inside a circle of radius a centered at $(x, y) = (-4a, 0)$ and is given by (see e.g. Meleshko and van Heijst 1994, van Heijst 2010)

$$\omega_{\text{dip}}(x, y, t = 0) = \begin{cases} \dfrac{2kU}{J_0(ka)} J_1(kr) \sin\theta & \text{if } 0 < r < a, \\ 0 & \text{if } r > a, \end{cases} \tag{2}$$

where

$$r = \sqrt{(x + 4a)^2 + y^2} \quad \text{and} \quad \sin\theta = \frac{y}{r}. \tag{3}$$

In (2) J_0 and J_1 are the zeroth and first order Bessel functions, respectively, and ka corresponds to the first zero of J_1 (i.e. $ka \simeq 3.83$). k is the arbitrary constant linearly relating the vorticity to the stream function (Meleshko and van Heijst 1994).
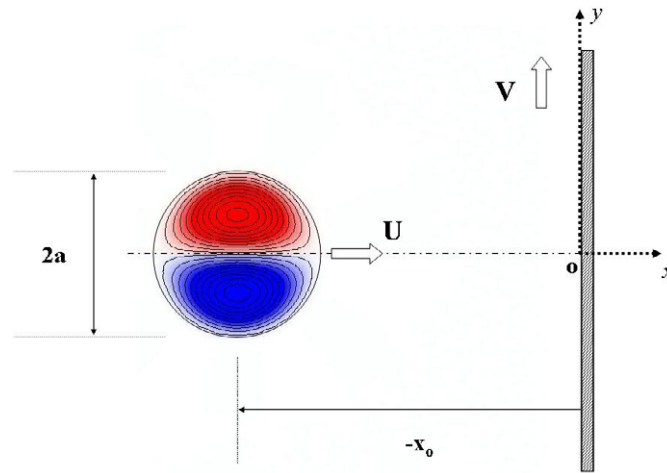
Figure 1. Geometry and flow configuration at $t = 0$. The circular domain of radius a denotes the region of the fluid with non-zero vorticity (positive and negative vorticity is denoted by red and blue, respectively) with contours indicating levels of constant vorticity. The vortex is initially located at $x_0 = -4a$ and moves in the positive x-direction with velocity U. The no-slip wall located at $x = 0$ starts moving at $t = 0$ with speed V in the positive y-direction.

For $t > 0$, up to the moment that it starts to interact with the wall, the dipole moves along a straight line (perpendicular to the wall) in the positive x-direction with initial speed U (> 0). As it evolves, its speed gradually decreases and its radius increases owing to viscous effects discussed by van Geffen and van Heijst (1998). After some time the dipole encounters the no-slip wall located at $x = 0$. This wall was started impulsively at $t = 0$ to slide parallel to itself with speed V in the positive y-direction.

The self-induced translation of the dipole and its subsequent collision with the sliding wall is governed by conservation of mass and momentum, which are described by

$$\nabla \cdot \mathbf{v} = 0, \tag{4}$$

$$\frac{\partial \mathbf{v}}{\partial t} + (\mathbf{v} \cdot \nabla)\mathbf{v} = -\frac{1}{\rho}\nabla p + \nu \nabla^2 \mathbf{v}, \tag{5}$$

respectively. Here ρ is the mass density and p is the pressure. The velocity $\mathbf{v}$ is related to the stream function ψ by

$$\mathbf{v} = \mathbf{e_z} \times \nabla \psi. \tag{6}$$

Moreover, ψ is related to the vorticity by

$$\omega = -\nabla^2 \psi. \tag{7}$$

By setting the initial diameter and speed of the Lamb–Chaplygin dipole equal to unity, and by measuring time in units of the advective time $2a/U$, we arrive at the following non-dimensional Navier–Stokes equation:

$$\frac{\partial \mathbf{v}}{\partial t} + (\mathbf{v} \cdot \nabla)\mathbf{v} = -\nabla p + \frac{1}{Re}\nabla^2 \mathbf{v}, \tag{8}$$

Table 1. Values of the control parameters, α and Re, used in the simulations.

| Simulation no. | $\alpha = \frac{V}{U}$ | Re | | Figure no. |
		(1×10^3)	(1×10^3)	
1	0.0	1	–	
2	0.5	1	10	2
3	1.0	1	–	
4	1.2	1	–	
5	1.3	1	–	
6	1.4	1	10	3
7	1.5	1	–	
8	2.0	–	10	
9	2.2	–	10	
10	2.4	–	10	
11	2.5	1	10	3
12	3.0	1	10	4

where Re is the Reynolds number based on the dipole characteristics, namely,

$$Re = \frac{2aU}{\nu}. \tag{9}$$

The total velocity field resulting from the evolving dipole and the sliding wall is solved numerically using the finite-element code COMSOL[3] on a computational domain that is bounded by the no-slip sliding wall at $x = 0$ (boundary condition here is $\mathbf{v} = (0, V)$ for $t \geqslant 0$). In order to reduce the impact of the other no-slip walls and associated vorticity production on the evolution of the dipole for the time interval considered, we assume a stress-free wall at $x = -15$ and periodicity along the y-direction with period 20. These values seem to be large enough, as has been checked with validation runs for $Re = 10^3$ for a domain with doubled width and period. Numerical simulations were performed for several values of the two control parameters that are Re and $\alpha = V/U$ (see table 1). Integrations were carried out with a second-order, backward-difference scheme and implicit time-stepping. Error control is enforced by prescribing a global tolerance of 1×10^{-3} on all variables. In order to improve the accuracy of the calculations, an ultra-fine triangular mesh was created near the no-slip wall, where the largest gradients occur. Typical element sizes in this region vary between 3×10^{-3} and 5×10^{-2} (normalized units). Coarser meshes with element sizes ranging from 5×10^{-2} to 6.7×10^{-1} were preferred close to the stress-free and periodic boundaries to reduce the computing time.

3. Results

3.1. General mechanisms

The results from the studies by Orlandi (1990) and by Kramer *et al* (2007) for dipole collisions with non-moving walls are first recalled. In the cases considered therein, vorticity is generated by the incoming dipole in the form of a boundary layer near the wall. As the boundary layer is advected by the primary dipole cores it detaches from the surface, leading to the formation of secondary vortices. Apparently, these newly formed dipoles are asymmetric, and therefore travel along curved trajectories, after some time leading to another collision. It must be noted that the entire process is symmetrical with respect to the dipole's symmetry axis.

---

[3] http://www.comsol.com

Apart from the dipolar vorticity distribution, the sliding wall itself acts as a source of additional vorticity: the wall vorticity introduced at $t = 0$ (when the wall starts moving) gradually diffuses from the wall into the bulk of the fluid. If we ignore the velocity field associated with the dipolar vorticity, this situation in fact corresponds to Stokes' first problem and, by using the dimensionless variables introduced before, the wall-induced vorticity is thus given by

$$\omega_{\mathrm{w}}(x, y, t) = \alpha \sqrt{\frac{Re}{\pi t}} \exp\left(-\frac{Re}{4t} x^2 \right) \tag{10}$$

for $x \leqslant 0$ and $t > 0$. This expression shows that for the Reynolds numbers considered in this study (see table 1) the timescale on which wall-induced vorticity diffuses into the fluid is much slower than the dipole's advective timescale. This implies that the vorticity generated by the wall and its associated velocity field do not influence the dipole's approaching path up to the time when it actually hits the wall (at $t \approx 1.5$). This is confirmed by our numerical computations that simulate the total flow field associated with the initial dipolar vorticity distribution (2) and the impulsively started sliding wall. However, it must be emphasized that the collisional and post-collisional evolution are decisively influenced by the sliding wall: the vortex structures evolve in an essentially asymmetric way, in contrast to the 'classical' rebound in the case of a non-sliding wall.

3.2. Asymmetric dipole–wall collision

The main finding of the present study is that the symmetry observed in the collision of a dipole with a non-sliding wall is broken once the wall slides parallel to itself. This situation is clearly illustrated in figures 2–4 in which we show snapshots of the numerically obtained vorticity fields for $Re = 10^3$ and 10^4, and for different wall speeds. For instance, figure 2 shows the asymmetric propagation of the secondary dipoles produced at the relatively low wall speed $\alpha = 0.5$.

In the case depicted in figure 3 for $\alpha = 3$, it is clearly seen that the dipole's upper half (containing vorticity of the same sign as the wall-induced vorticity) is incapable of producing sufficiently strong oppositely signed vorticity at the wall to form a secondary dipole. Instead, this dipole core tends to remain attached to the sliding wall and translates along it with a speed that is, nonetheless, lower than the wall velocity. There is a critical wall speed $\alpha = \alpha_{\mathrm{crit}}$ above which this attachment is observed, whereas for $0 < \alpha < \alpha_{\mathrm{crit}}$ the dipole's upper half is still capable of producing sufficiently strong negative vorticity to overcome the wall-induced positive vorticity.

Between these two regimes, when $\alpha \approx \alpha_{\mathrm{crit}}$, an intermediate scenario is observed (figure 4). In this transitional regime the upper half of the dipole is still able to produce and scrape off some oppositely signed (negative) vorticity from the wall. However, the amplitude of this vorticity is insufficient to favor a full detachment. Instead, the negative vorticity is wrapped around the core forming a ring of negative vorticity. As a result, this *shielded* monopolar vortex remains close to the wall and propagates parallel to its surface with a speed lower than α.

In order to obtain a quantitative estimate for α_{crit} it is useful to plot the distance D to the wall of the dipole's upper core as time progresses with

$$D(t) = \frac{\int_A x\, \omega\, \mathrm{d}x\, \mathrm{d}y}{\Gamma} \quad \text{for } \omega \geqslant 0, \tag{11}$$
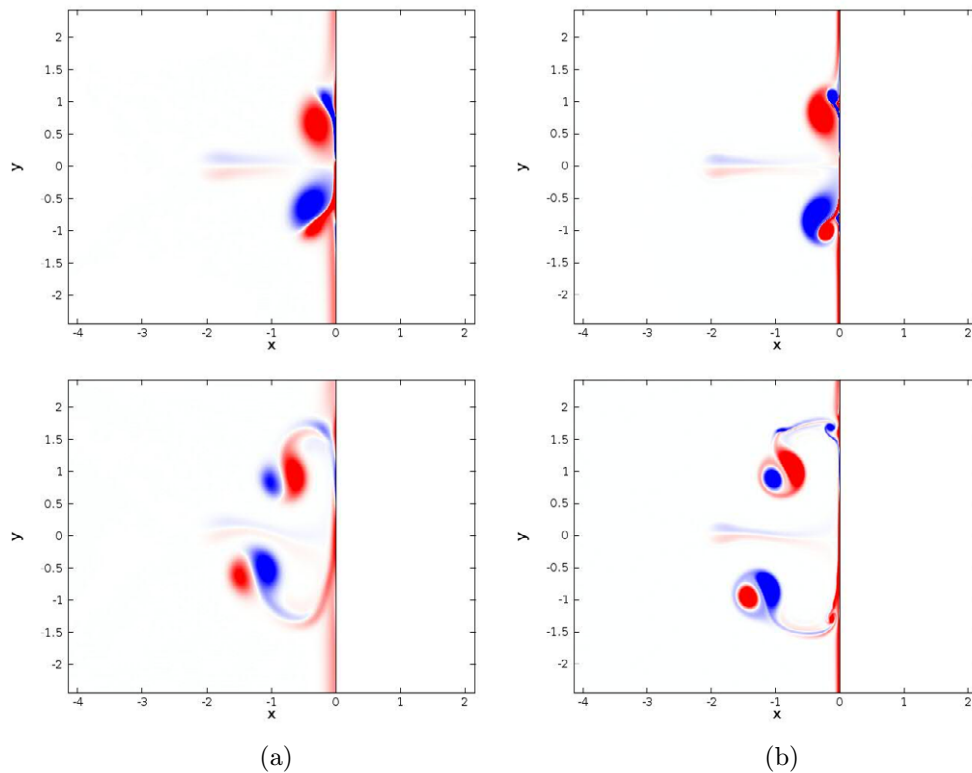
Figure 2. Vortex interaction with a wall moving at the sub-critical speed $\alpha = 0.5$ for times $t = 2.6$ (upper row) and $t = 4.5$ (lower row). Columns (a) and (b) show the evolution of the vorticity field for $Re = 10^3$ and 10^4, respectively.

where $\Gamma = \int_A \omega \, dx \, dy$ is the circulation calculated over the surface A occupied by the positive core.

Figure 5 shows plots of D for various values of the wall velocity α for the case $Re = 10^3$. Consistent with previous arguments, it is observed that the dipole approaches the sliding wall at a constant speed (roughly equal to 1) unperturbed by the wall and its related vorticity effects. The actual interaction starts at around $t \approx 1.5$ and the characteristic evolution that follows depends on the magnitude of α. In particular, at $\alpha = 0.5$ the rebound of the corresponding core is clearly seen. On the other hand, for $\alpha = 3$ such a rebound is completely absent and the distance of the core centroid to the surface remains approximately constant. It may be surmised that the rate of decrease of the distance to the wall will be dictated essentially by diffusive effects.

Also, from this figure a rough estimate for the critical wall speed α_{crit} may be obtained by looking at the curves' inflection points. A rebound of the dipole takes place if the corresponding trajectory shows a point of inflection (at $t \approx 2.2$), whereas no rebound occurs if such a point is absent. This is clearly seen in figure 5 for the trajectories corresponding to $\alpha_{\text{crit}} = 0.5$ and 3, respectively. Therefore, and also from visual inspection of the vorticity plots, we estimate the critical value of the wall speed to be roughly $\alpha_{\text{crit}} \approx 1.4$ for $Re = 10^3$. If the Reynolds number is increased from 10^3 to 10^4, the critical wall speed increases slightly, as can be seen in figure 6. In this case the critical α-value is estimated to be $\alpha_{\text{crit}} \approx 2.5$. Higher
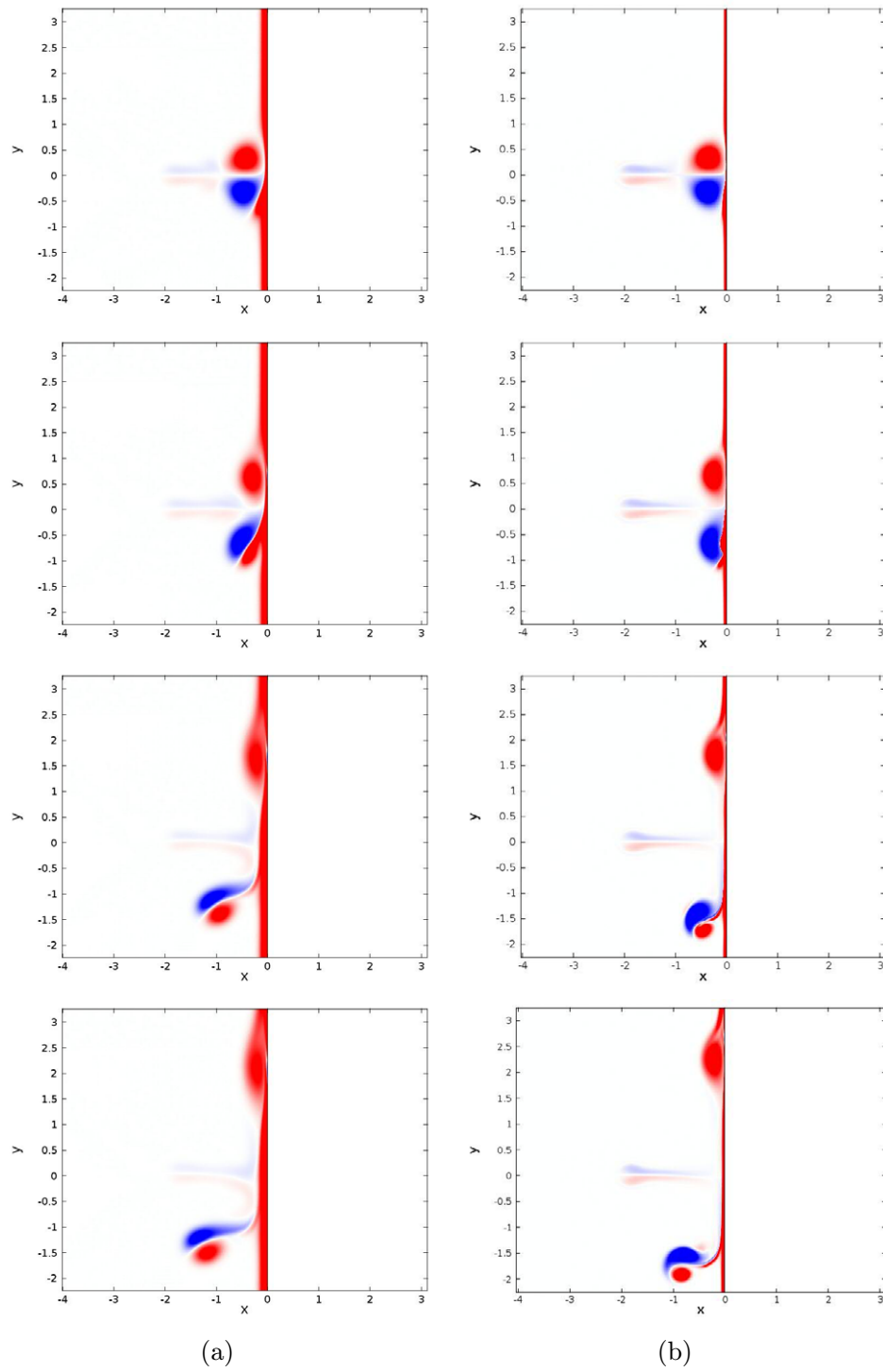
Figure 3. Vortex interaction with a wall moving at the super-critical speed $\alpha = 3$ for times $t = 1.9$, 2.4, 3.5 and 4 (time increases from the top row to the bottom row). Columns (a) and (b) show the evolution of the vorticity field for $Re = 10^3$ and 10^4, respectively.
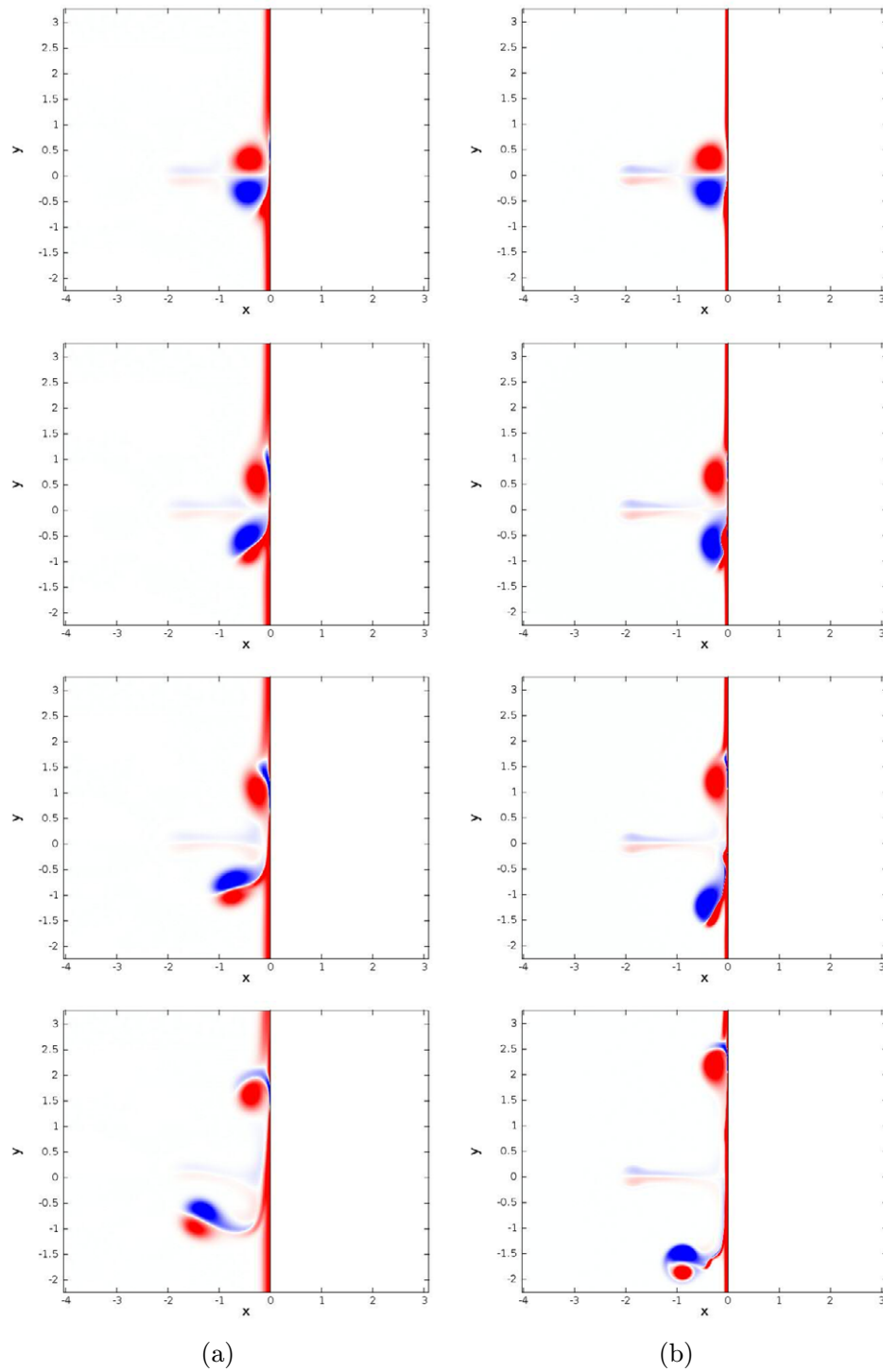
(a)   (b)

Figure 4. Vortex collision with a wall moving at critical speed for times $t = 1.9$, 2.4, 3 and 4 (time increases from the top row to the bottom row). Column (a) shows the evolution of the vorticity field for $\alpha_{crit} = 1.4$ at $Re = 10^3$; column (b) shows the evolution for $\alpha_{crit} = 2.5$ at $Re = 10^4$.
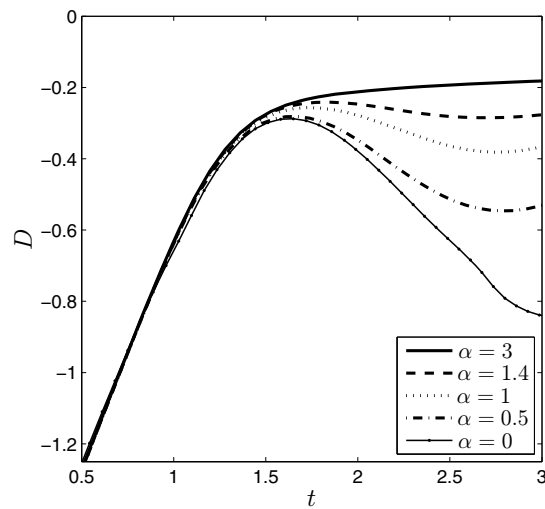
Figure 5. Evolution of the horizontal distance to the wall D of the positive dipole core, for $Re = 10^3$ and different wall velocities.
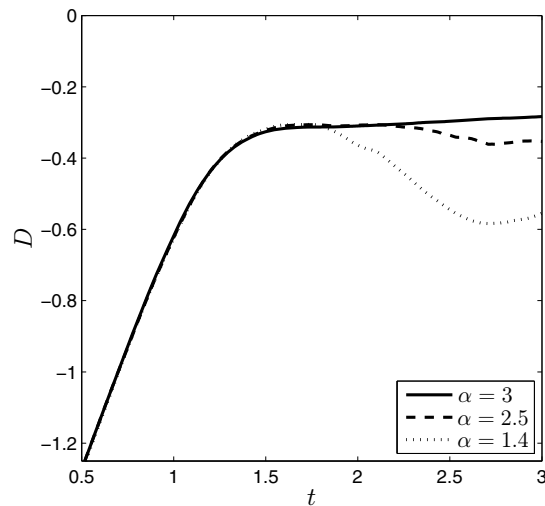

Figure 6. Evolution of the horizontal distance to the wall D of the positive dipole core, for $Re = 10^4$ and wall velocities near α_{crit}.

values of α_{crit} for increasing Re seem plausible, since higher Re-values also imply higher amplitude vorticity filaments detaching from the wall (Kramer *et al* 2007).

In the $\alpha > \alpha_{\text{crit}}$ regime the temporal evolution of the lower dipole half (containing negative vorticity) also shows some specific behavior which depends on the Reynolds number (figure 3). For instance, when $Re = 10^3$ the secondary vortex will continue to propagate along a straight path away from the wall, while for $Re = 10^4$ it will move along a curved trajectory. Generally speaking, at higher Reynolds numbers the filaments and other small-scale eddies with positive and negative vorticity develop into more compact structures, as can be seen in figure 4 (e.g. Kramer *et al* 2007).

3.3. Analytical estimate for α_{crit}

Apart from the numerically obtained value, it is also possible to analytically estimate the critical wall velocity, α_{crit}, above which one of the dipole's halves does not rebound. For that purpose, we assume that the exterior flow field of the approaching dipole is given by the potential flow generated by two *infinitely* long cylinders (of unit radius), symmetrically located on opposite sides of the sliding wall and moving along the x-axis with unit speed toward the wall. Then, by standard potential flow theory, such a flow is dictated by the following stream function in the laboratory frame-of-reference:

$$\psi_{cyl} = \frac{y}{4}\left[\frac{1}{(2-t+x)^2+y^2} - \frac{1}{(2-t-x)^2+y^2}\right] \tag{12}$$

for $0 \leqslant t < 1.5$, where we have assumed that at $t = 0$ the position of the cylinder in the half-plane $x < 0$ coincides with the position of the Lamb–Chaplygin dipole. Such an approximation does have its limitations, however, since we ignore the influence of the velocity field created by the moving wall on the approaching dipole. According to previous arguments, this appears to be legitimate up to the moment at which the dipole starts to interact with the wall (i.e. at $t \approx 1.5$).

Although the stream function (12) gives rise to a zero normal velocity at $x = 0$, the velocity tangential to the wall, given by

$$v(x=0, y, t) = -\left.\frac{\partial \psi_{cyl}}{\partial x}\right|_{x=0} = \frac{y\,(2-t)}{[(2-t)^2+y^2]} \tag{13}$$

in the interval $0 \leqslant t < 1.5$, is not zero.

Precisely, this non-vanishing tangential flow at the wall produces the oppositely signed vorticity in the boundary layer that will compete with the positive vorticity induced by the sliding wall. Therefore, it may be conjectured that the positive dipole half will not rebound from the sliding wall if the velocity of the wall is everywhere at least as large as the tangential velocity given by (13) at the instant when the dipole starts to interact with the wall, i.e. $\alpha \geqslant |v(x=0, y, t=1.5)|$. Under such circumstances, the collision of the upper core will not lead to the production of negative vorticity at the wall and no rebound will occur. This condition is satisfied if

$$\alpha \geqslant \alpha_{crit} = \max[v(x=0, y, t=1.5)] \simeq 1.3. \tag{14}$$

The obtained result does not depend on the Reynolds number, whereas the numerical simulation indicates a weak dependence of α_{crit} on Re. Moreover, we ignored any viscous effects in the dipole's motion toward the wall up to the time $t = 1.5$, at which we assume these effects to become active instantaneously. Nevertheless, the above derived value for α_{crit} is of the same order of magnitude as the numerically observed values. In summary, one could conclude that a rebound of one of the two dipole cores is suppressed if the wall speed is at least of the same order of magnitude as the translation speed of the dipole, provided the Reynolds number is sufficiently large.

4. Conclusions

Perpendicular collisions of dipolar vortices with sliding walls have been investigated numerically. By virtue of the no-slip condition a wall moving at constant speed V introduces

vorticity that diffuses into the fluid and, upon collision of the dipole with the wall, breaks the symmetry of the initial vorticity distribution about the mid-line of the vortex. The numerical results indicate that the evolution of the flow is essentially determined by V. In fact, a critical wall speed has been identified which marks the transition between two distinctive regimes. Below this critical speed the generation of a pair of secondary vortices that rebound away from the wall is observed. In contrast, the blending of one of the primary cores with the boundary layer is the defining feature of the asymmetrical behavior observed in super-critical regimes. Such a blending occurs for the core containing vorticity of the same sign as that of the boundary layer.

In general terms the Reynolds number has a limited effect during the initial stages of the process. However, depending on the value of Re, the filaments and small eddies are susceptible to decay at different rates. Moreover, near the transitional regime Re has a subtle influence on the collision behavior, which entails a change in the critical value of α_{crit}. According to the simulations this critical speed varies in the range $1.4 \leqslant \alpha_{\text{crit}} \leqslant 2.5$ when $10^3 \leqslant Re \leqslant 10^4$.

The present study into the collision of dipoles with a no-slip wall is relevant for many situations where asymmetry is introduced in the temporal evolution of such interaction due to moving walls, or due to cross-flows, and may help to better parameterize these asymmetries, which are encountered in many practical applications.

Acknowledgments

References

Atassi O V, Bernoff A J and Lichter S 1997 The interaction of a point vortex with a wall-bounded vortex layer *J. Fluid Mech.* **343** 169–95

Carnevale G F, Velasco Fuentes O U and Orlandi P 1997 Inviscid dipole-vortex rebound from a wall or coast *J. Fluid Mech.* **351** 75–103

Chuang F S and Conlisk A T 1989 The effect of interaction on the boundary layer induced by a convected rectilinear vortex *J. Fluid Mech.* **200** 337–65

Danaila I 2004 Vortex dipoles impinging on finite aspect ratio rectangular obstacles *Flow Turbul. Combust.* **72** 391–406

Doligalski T L and Walker J D A 1984 The boundary layer induced by a convected two-dimensional vortex *J. Fluid Mech.* **139** 1–28

Geffen J H G M and van Heijst G J F 1998 Viscous evolution of 2D dipolar vortices *Fluid Dyn. Res.* **22** 191–213

Holzäpfel F and Steen M 2007 Aircraft wake-vortex evolution in ground proximity: analysis and parameterization *AIAA J.* **45** 218–27

Kramer W, Clercx H J H and van Heijst G J F 2007 Vorticity dynamics of a dipole colliding with a no-slip wall *Phys. Fluids* **19** 126603

Loerakker S, Cox L G E, van Heijst G J F, de Mol B A J M and van de Vosse F N 2008 Influence of dilated cardiomyopathy and a left ventricular assist device on vortex dynamivs in the left ventricle *Comput. Methods Biomech. Biomed. Eng.* **11** 649–60

Meleshko V V and van Heijst G J F 1994 On Chaplygin's investigations of two-dimensional vortex structures in an inviscid fluid *J. Fluid Mech.* **272** 157–82

Orlandi P 1990 Vortex dipole rebound from a wall *Phys. Fluids* A **5** 1429–36

Orlandi P 1993 Vortex dipoles impinging on circular cylinders *Phys. Fluids* A **9** 2196–206

Peridier V J, Smith F T and Walker J D A 1991a Vortex-induced boundary-layer separation: Part 1. The unsteady limit problem $Re \rightarrow \infty$ *J. Fluid Mech.* **232** 99–131

Peridier V J, Smith F T and Walker J D A 1991b Vortex-induced boundary-layer separation: Part 2. Unsteady interacting boundary-layer theory *J. Fluid Mech.* **232** 133–65

van Heijst G J F 2010 *Dynamics of Vortices in Rotating and Stratified Fluids* (*Lecture Notes in Physics* vol 805) ed J-B Flór (Berlin: Springer) pp 1–34

Verzicco R, Flór J B, van Heijst G J F and Orlandi P 1995 Numerical and experimental study of the interaction between a vortex dipole and a circular cylinder *Exp. Fluids* **18** 153–63

Zheng Z C and Ash R L 1996 Study of aircraft wake vortex behavior near the ground *AIAA J.* **34** 580–89